ELSEVIER

Polymer 41 (2000) 3925–3935

polymer

Kinetic modeling of free radical polymerization of styrene initiated by the bifunctional initiator 2,5-dimethyl-2,5-bis(2-ethyl hexanoyl peroxy)hexane☆

L. Cavin, A. Rouge, Th. Meyer*, A. Renken

Laboratory of Chemical Reaction Engineering, Swiss Federal Institute of Technology, CH-1015 Lausanne, Switzerland

Received 30 April 1999; received in revised form 3 September 1999; accepted 10 September 1999

Abstract

This paper deals with the kinetic study of bulk free radical polymerization of styrene initiated with the commercial bifunctional initiator 2,5-dimethyl-2,5-bis(2-ethyl hexanoyl peroxy)hexane (Lupersol 256). The polymerization kinetics is investigated by DSC measurement for temperatures between 80 and 110°C and for initiator initial concentration from 0.115 up to 0.46 mol%. The experimental conversion and reaction rate are compared and discussed with the calculated values. For modeling the polymerization rate, a reaction scheme similar to the one given by Yoon and Choi (Polymer 1992;33(21):4582–4591) has been used and adapted. A detailed diffusional and semi-empirical model proposed by Chiu et al. (Macromolecules 1983;16(3):348–357) has been modified by Rouge (Etude de la polymérisation radicalaire du styrène initiée par un amorceur bifonctionnel dans un réacteur tubulaire à recyclage, Diploma work, DC, EPF, Lausanne, 1997) in order to describe these results. The model allows the description of the number molecular weight, but the polydispersity is underestimated for conversion higher than 70%. For temperature higher than 100°C, thermal initiation must be taken into account. The efficiency factor is found close to 1, but seems to decrease for temperatures above 100°C.

Keywords: Bulk free radical styrene polymerization; Symmetrical bifunctional initiator; Diffusion termination

1. Introduction

Due to the nature of free radical polymerization, it is not possible to obtain high polymerization rates and simultaneously a high molecular weight in bulk or solution processes. The problem can be overcome by using multifunctional initiators and by controlling the decomposition rate of the labile groups [2]. Comparison of monofunctional systems with bifunctional can be found in the literature [3–8]. The presence of a second radical generating function distributed in the growing and dead polymer can be engaged in further initiation, propagation, chain transfer and termination reaction during the course of polymerization. Thus, bifunctional initiators appear to be a new alternative to control efficiently the molecular weight and monomer conversion. However, the presence of those additional functional groups leads to rather complex polymerization kinetics.

In order to use efficiently initiators during the polymerization of styrene in a continuous reactor, it is necessary to propose a kinetic model and to validate it by experimental measurements. A mathematical model for the polymerization of styrene initiated with symmetrical bifunctional initiator is described. Predicted polymerization rates and polymer molecular weight are compared with experimental data.

Generally, there are two kinds of bifunctional initiators: the symmetrical one with two identical labile groups having the same thermal stability and the unsymmetrical one having labile groups with different thermal stabilities. Studies of batch bulk polymerization of styrene initiated with symmetrical [8–10], with unsymmetrical [7], with a mixture of symmetrical [5] and even recently with a mixture of mono and bifunctional initiator have been performed [6]. The interest of such investigations is the development of kinetic models allowing the description of the experimental results and the optimization of new polymerization routes.

There is also an interest in using polyfunctional initiators to produce polymers of tuned properties. Kim [11] analyzed the steady state behavior of a CSTR for the bulk polymerization of styrene initiated with a symmetrical bifunctional initiator.

☆ Presented at the 1999 Spring AIChE Meeting, Polymer Reaction Engineering.

* Corresponding author.

0032-3861/00/$ - see front matter
PII: S0032-3861(99)00651-5

Nomenclature

a,b	Parameter for the gel effect
E	Letter representing any moment or any concentration (mol m^{-3})
f	Efficiency factor for the initiator
I	Initiator concentration (mol m^{-3})
$\overline{IP}$	Polydispersity index
k_d	Decomposition constant (s^{-1})
k_i	Initiation constant ($m^3\ mol^{-1}\ s^{-1}$)
k_p	Propagation constant ($m^3\ mol^{-1}\ s^{-1}$)
k_t	Termination constant ($m^3\ mol^{-1}\ s^{-1}$)
k_{t0}	Termination constant without gel effect ($m^3 mol^{-1} s^{-1}$)
M	Monomer concentration (mol m^{-3})
M'	Concentration in chain with two dead ends (with subscript) (mol m^{-3})
MM_s	Molecular mass of styrene (g mol^{-1})
$\bar{M}_n$	Average number molecular weight (g mol^{-1})
$\bar{M}_w$	Average mass molecular weight (g mol^{-1})
P	Concentration in chain with one dead end and a radical group (mol m^{-3})
Q	Concentration in chain with one radical end and one peroxide group (mol m^{-3})
R	Concentration in acyloxy radical (mol m^{-3})
R'	Concentration in diradical (mol m^{-3})
R_A	Concentration in peroxide radical (mol m^{-3})
R_E	Reaction rate of E (mol $m^{-3}\ s^{-1}$)
S	Concentration in chain with two radical ends (with subscript) (mol m^{-3})
t	Time (s)
$t_{1/2}$	Half-life time (s)
T	Temperature (K)
U	Concentration in chain with two peroxides (with subscript) (mol m^{-3})
V	Volume (m^3)
X	Conversion
Z	Concentration in chain with one dead end and one peroxide (with subscript) (mol m^{-3})
[–OO–]	Concentration of peroxide group on the initiator, Q, U or Z (mol m^{-3})
ε	Volume contraction factor
θ_t	Parameter for the gel effect, empirical diffusional model (s mol m^{-3})
θ_t'	Parameter for the gel effect, model of Chiu [1] (s)
λ_0	Total concentration in radical (mol m^{-3})
$\lambda_{\xi,k}$	k order moment of the ξ species (mol m^{-3})
ξ	Species P, Q, S, U, Z or M' with subscript: concentration of P, Q, S, U, Z or M' (mol m^{-3})
ϕ	Volume fraction

Subscripts

0	At the beginning of the reaction
1	Containing 1 molecule of monomer
k	Order of the moment of a species
m	Containing m molecules of monomer
M	For the monomer
n	Containing n molecules of monomer
S	For the styrene
t	Overall (every length mixed up)

Abbreviations

c.m.	Complete model
DSC	Differential Scanning Calorimetry
Lu256	Lupersol 256: 2,5-dimethyl-2,5-bis(2-ethyl hexanoyl peroxy)hexane
QSSA	Quasi-steady-state assumption

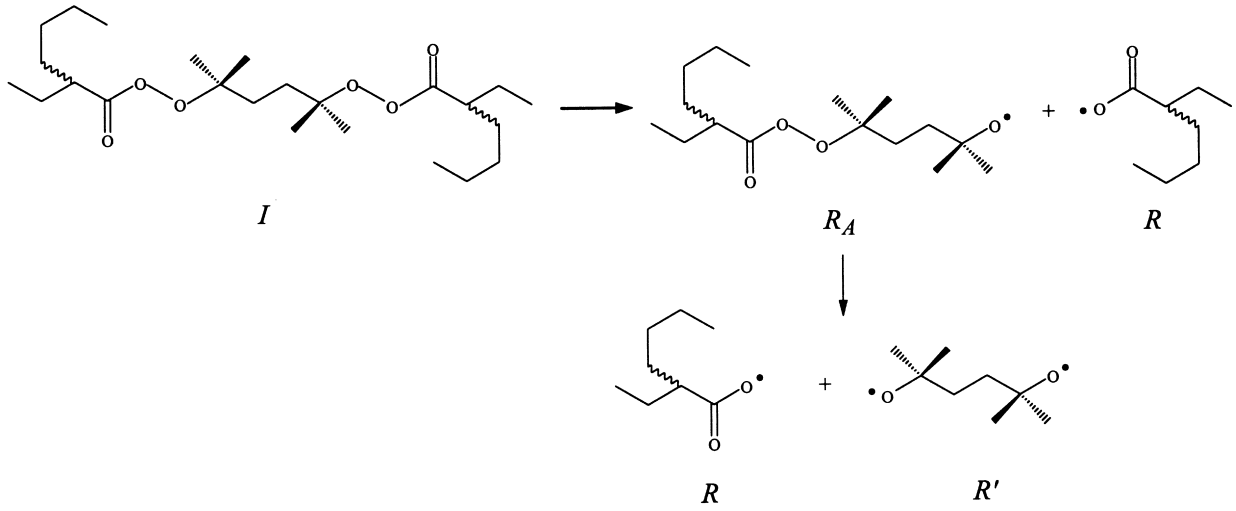

Fig. 1. Decomposition of the initiator Lu256.

Yoon [12] studied the free radical solution polymerization of styrene initiated with a binary mixture of symmetrical bifunctional initiators in a tubular reactor filled with static mixers. A dynamic axial dispersion model was used to investigate the transient behavior of the reactor.

2. Theoretical

2.1. Kinetic modeling

A reaction scheme similar to the one given by Yoon [9] has been used and adapted. The different steps occurring during the polymerization of styrene with bifunctional initiator are identical as for a monofunctional initiator.

The chemical structure and the decomposition of the symmetrical bifunctional initiator 2,5-dimethyl-2,5-bis(2-ethyl hexanoyl peroxy)hexane (Lu256) is presented in Fig. 1. Increasing the temperature leads to the homolytic decomposition of the oxygen–oxygen bond of the first peroxide giving two monoradicals: one containing an undecomposed peroxide and the other without. The monoradical containing a peroxide group can be integrated in a polymer chain, and after termination can lead to a momentarily inactive chain. It can be then decomposed, leading to a new active chain, which can undergo a new cycle of initiation, propagation and termination. Globally, each initiator molecule decomposes two times to give two monoradicals and one diradical.

Due to the presence of a second labile group in the initiator molecule, the kinetic scheme becomes more complicated and their end types distinguish the different species involved during the polymerization as shown on Fig. 2.

The subscript n indicates the number of repeating units in the polymer chain. The polymeric species Q_n, U_n and Z_n contain one or two undecomposed peroxide groups, which are subject to further decomposition reactions. The kinetic scheme is described in Table 1, under the following assumptions:

- The concentration of polymeric diradical species S_n is three orders of magnitude smaller than the polymeric monoradicals P_n and Q_n [1–14]. The diradical species S_n could then be neglected [3,4,6,8,10] (Fig. 3) leading to the simplified model used for all our simulations. The complete model is presented with an annotation (c.m.) after each equation to indicate where it can by simplified.
- The decomposition rate constant is assumed to be unaffected by the neighboring groups [15,16]. The probability of the cleavage of the two bonds is identical due to the symmetrical structure of the initiator [14,17,18]. Initiator with two decomposition constants would also leads to a bimodal molecular weight distribution and to a break in the curve of polymer accumulation [15,16,18], which is not experimentally observed. It is also assumed that the thermal stability of the peroxide group in the polymer chains is independent of the chain length.
- The initiator efficiency is taken as constant during the polymerization and close to 1 (Fig. 10). As there is no

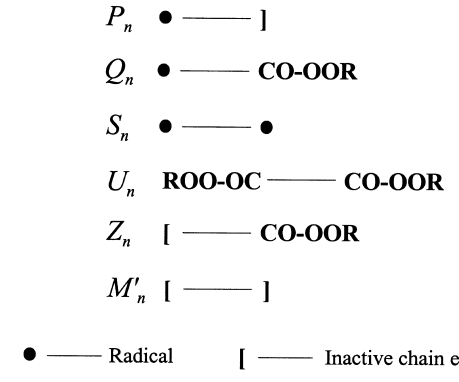

Fig. 2. Polymeric species in free radical styrene polymerization initiated with bifunctional initiator.

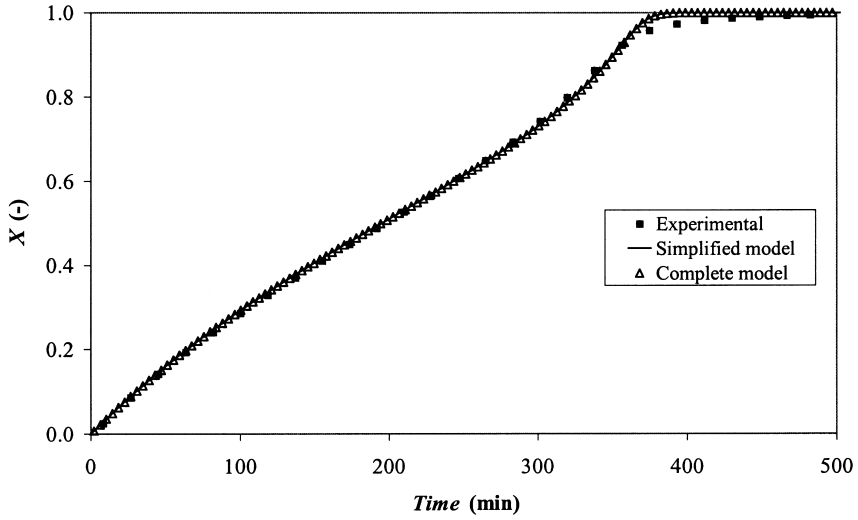

Fig. 3. Influence of the diradical species S_n on the simulation. $T = 80°C$, $I_0 = 0.115$ mol%, simplified and complete model.

evidence of a partial efficiency, it has been used to fix the parameter a, b and θ_t in our termination model and then has been optimized (Table 4).

- Thermal initiation and chain transfer reactions are neglected. As mentioned by Fried [19] and Kukulj [20], the chain transfer constant is in a range of 10 000 smaller than the propagation constant.
- The termination rate constant is identical for all macroradical species.
- The termination step occurs only by combination [21,22].
- The radical species R, R_A and R' do not participate in the termination process. According to Bamford [23] there are three sources of radical wastage. The first is through recombination of primary radicals. The second is the termination of growing chain by a primary radical, which is usually observed at high rates of initiation or low monomer conversion. The third is the recombination of primary radicals derived from the same molecule of initiator, or geminate recombination. But this corresponds to a lower decomposition constant, rather than a lower efficiency.

Table 1
Kinetic scheme of the free radical styrene polymerization initiated with symmetrical bifunctional initiator

—Peroxide decomposition, k_d being the peroxide decomposition constant:

$I \xrightarrow{2k_d} R + R_A$
$R_A \underset{k_d}{\xrightarrow{k_d}} R + R'$ (c.m.)
$Q_n \xrightarrow{2k_d} S_n + R$ $n \geq 1$ (c.m.)
$U_n \xrightarrow{k_d} Q_n + R$ $n \geq 2$
$Z_n \xrightarrow{} P_n + R$ $n \geq 1$

—Initiation, k_i being the initiation constant:

$R + M \xrightarrow{k_i} P_1$
$R_A + M \xrightarrow{k_i} Q_1$
$R' + M \xrightarrow{2k_i} S_1$ (c.m.)

—Propagation ($n \geq 1$), k_p being the propagation constant:

$P_n + M \xrightarrow{k_p} P_{n+1}$
$Q_n + M \underset{2k_p}{\xrightarrow{k_p}} Q_{n+1}$
$S_n + M \xrightarrow{2k_p} S_{n+1}$ (c.m.)

—Termination ($n, m \geq 1$), k_t being the termination constant:

$P_n + P_m \underset{k_t}{\xrightarrow{k_t}} M'_{n+m}$
$P_n + Q_m \underset{2k_t}{\xrightarrow{k_t}} Z_{n+m}$
$P_n + S_m \xrightarrow[k_t]{} P_{n+m}$ (c.m.)
$Q_n + Q_m \xrightarrow{2k_t} U_{n+m}$
$Q_n + S_m \xrightarrow{4k_t} Q_{n+m}$ (c.m.)
$S_n + S_m \xrightarrow{} S_{n+m}$ (c.m.)

2.2. Kinetic equations

The evolution of the concentration of each species shown on Fig. 2 is obtained by numerical integration of the differential moment equations. The k-order moment of one species in solution is defined as follows [24]:

$$\lambda_{\xi,k} = \sum_{n=j}^{\infty} n^k \xi_n \qquad \xi = P, Q, S, U, Z \text{ or } M'$$

$$j = 1 \text{ for } P, Q, S, Z \qquad \text{and } j = 2 \text{ for } M', U \tag{1}$$

$\lambda_{\xi,k}$ is the k-order moment of the species ξ. For instance, the 0-order moment represents the overall concentration of one

Table 2
Kinetic constants and gel effect

	Empirical diffusional model
k_d (s^{-1})	$k_d = 2.085 \times 10^{15}\ e^{(-15957/T)}$ [34]
f	$f = 1$ (before optimization)
k_i, k_p ($m^3\ mol^{-1}\ s^{-1}$)	$k_i = k_p = 105 \times 10\ e^{(-3554/T)}$ [26,27]
k_t ($m^3\ mol^{-1}\ s^{-1}$)	$\frac{1}{k_t} = \frac{1}{k_{t0}} + \frac{\theta_t}{e^{(-1/(a+b\varphi_M))}}$ $a = 2.2 \times 10^{-4} T - 0.0214$ $b = 0.094 + 7.45 \times 10^{-5}$[–OO–] $\theta_t = e^{(6803/T)} 4.155 \times 10^{-18} (1 + \frac{1}{\sqrt{[\text{–OO–}]}})$ $k_{t0} = 1.255 \times 10^6\ e^{(-846/T)}$ [26,27]

Table 3
Half-life time of Lupersol 256 with temperature

T (°C)	$t_{1/2}$ (min)	
	Ref. [34]	Our results
80	237.2	214.2
90	68.3	63.1
100	21.0	19.8
110	6.9	6.6

species, every length mixed up. It is simply noted ξ_t. The reaction rates of the initiator, monomer and of the different species are reported in Appendix A.

The concentration of R, R' and R_A are calculated with the quasi-steady-state assumption (QSSA):

$$R_A = \frac{2fk_dI}{k_d + k_iM} \qquad R' = \frac{fk_dR_A}{2k_iM} \qquad \text{(c.m.)}$$
$$R = \frac{fk_d}{k_iM}(2I + R_A + Q_t + 2U_t + Z_t) \qquad \text{(c.m.)} \tag{2}$$

The volume can be expressed as a function of the conversion of monomer and the volume contraction factor ε:

$$\varepsilon = \frac{V_{X=1} - V_{X=0}}{V_{X=0}} \tag{3}$$

$$V = V_0(1 + \varepsilon X) \qquad \frac{dV}{dt} = V_0\varepsilon\frac{dX}{dt} \tag{4}$$

The variation of the concentration of the initiator, monomer, as well as the 0, 1st and 2nd order moment of each species are calculated from the reaction rate and the volume variation:

$$\frac{dE}{dt} = R_E - E\frac{dV}{Vdt} \qquad E = \lambda_{\xi,k}, I, M \tag{5}$$

The monomer concentration and the rate of monomer disappearance are defined as following:

$$M = M_0\frac{1 - X}{1 + \varepsilon X} \tag{6}$$

$$-R_M = \frac{dX}{dt}\frac{M_0}{1 + \varepsilon X} \tag{7}$$

If the consumption of monomer during the initiation is neglected, the overall polymerization rate is equal to the propagation constant multiplied by the monomer concentration and by the total concentration of radicals:

$$-R_M = k_pM(P_t + Q_t + 2S_t) \qquad \text{(c.m.)} \tag{8}$$

Under the QSSA and by the iso-reactivity of radicals, the total concentration of radicals can be estimated and the overall polymerization rate can be written as:

$$-R_M = k_p\sqrt{\frac{2fk_d[\text{–OO–}]}{k_t}}M \tag{9}$$

[–OO–] can be expressed as a function of the initial concentration of peroxide groups $[\text{–OO–}]_o$, and so as a function of the initial initiator concentration I_0, time t and conversion X. One peroxide group giving two radicals, thus:

$$[\text{–OO–}] = \frac{2I_0\,e^{-k_dt}}{1 + \varepsilon X} \tag{10}$$

Finally, by correct substitution, the variation of the conversion as a function of the conversion becomes:

$$\frac{dX}{dt} = k_p\sqrt{\frac{4fI_0k_d\,e^{-k_dt}}{k_t(1 + \varepsilon X)}}(1 - X) \tag{11}$$

2.3. Gel effect and kinetic constants

The empirical gel effect used by Yoon [9] does not allow the modeling of our results for the reaction rate dX/dt (Fig. 7). So, in order to account for the gel effect, a diffusion model taken from the literature and then modified by

Table 4
Measured and predicted average molecular weights in number, measured average molecular weights in mass and optimized initiator efficiency

T (°C)	I_0 (mol%)	f	$\bar{M}_n$ (g mol^{-1})		$\bar{M}_w$ (g mol^{-1})
		Optimized	Measured	Predicted	Measured
80	0.244 (AIBN)		62 000	43 600[a]	260 000
80	0.115	0.96	92 000	108 000	332 000
80	0.230	0.96	61 800	67 900	209 700
80	0.460	0.94	34 000	35 800	132 800
90	0.115	0.96	65 600	96 700	229 000
90	0.230	0.95	39 900	52 800	142 000
90	0.460	0.94	27 000	27 100	110 000
100	0.115	0.99	58 000	87 900	196 000
100	0.230	0.95	35 200	49 000	149 000
100	0.460	1.00	22 500	23 800	82 000
110	0.460	0.80	19 500	22 000	78 100

[a] Calculated with $f = 1$.

Rouge [13] is taken. The expression proposed by Chiu [1] (for the methyl methacrylate) is the following:

$$\frac{1}{k_t} = \frac{1}{k_{t0}} + \frac{\theta'_t}{\frac{\phi_M}{e^{a+b\phi_M}}}\lambda_0 \tag{12}$$

λ_0 is the concentration in radical, ϕ_M is the volume fraction of monomer. The parameters are: a depending on the temperature, b fixed and θ'_t function of the temperature and initial initiator concentration, I_0. The relationship between θ'_t and I_0 allows to take into account the chain length (the smaller I_0, the higher the chain length). However, it is difficult to understand why the radical concentration can modify the rate law. For a reaction limited only by the diffusion, the equation becomes:

$$-R_{\lambda_0} = \frac{e^{\frac{\phi_M}{a+b\phi_M}}}{\theta'_t}\lambda_0 \tag{13}$$

It is a first-order equation, whereas the diffusion limited rates are second order [25].

Therefore in our model, the following expression, similar to that of Chiu [1], but in which the λ_0 does not intervene and in which θ_t has not the same unit as θ'_t, is used:

$$\frac{1}{k_t} = \frac{1}{k_{t0}} + \frac{\theta_t}{\frac{-1}{e^{a+b\phi_M}}} \tag{14}$$

In order to better describe the measurements, k_t has to be varied as a function of a parameter other than the temperature. The instantaneous peroxide concentration does not depend on the polymerization history and is chosen for this reason instead of the initial concentration of initiator. k_{to} is taken in the literature [26,27] and f is fixed to be 1.

First, a and b parameters are adjusted from the experimental results by a trial and error adjustment. Constant values are momentarily fixed for these two parameters. Then θ_t is adjusted so that it fits the experimental results and the dependency with the temperature and peroxide concentration is found. Then the dependencies of a with the temperature and b with the temperature and peroxide concentration are found. Then a, b and θ_t are adjusted. Finally, f is optimized.

The values of the coefficients and parameters for the termination constant and the values for others kinetic constants are taken from the Table 2.

2.4. Average molecular weights

The quality of the polymer is defined by its mass and number molecular weight, and its polydispersity index, which can all be calculated using the moments defined above. The number average molecular weight represents the mass of polymer divided by the number of chains, or the average mass of a chain taken at random:

$$\bar{M}_n = \frac{\sum_\xi \lambda_{\xi,1}}{\sum_\xi \lambda_{\xi,0}} MM_S \tag{15}$$

The mass-average molecular weight is the average mass of the chain containing a monomer taken at random:

$$\bar{M}_w = \frac{\sum_\xi \lambda_{\xi,2}}{\sum_\xi \lambda_{\xi,1}} MM_S \tag{16}$$

And the polydispersity index is the ratio of these two averages:

$$\overline{IP} = \frac{\bar{M}_w}{\bar{M}_n} \tag{17}$$

3. Materials and methods

The isothermal radical polymerization of styrene at 80, 90, 100 and 110°C and the decomposition of the bifunctional initiator diluted at 10 vol%. in ethylbenzene were investigated with a Mettler DSC 27HP (Greifensee, Switzerland) differential scanning calorimeter (DSC). The calorimeter was calibrated with reference to the melting heat of indium.

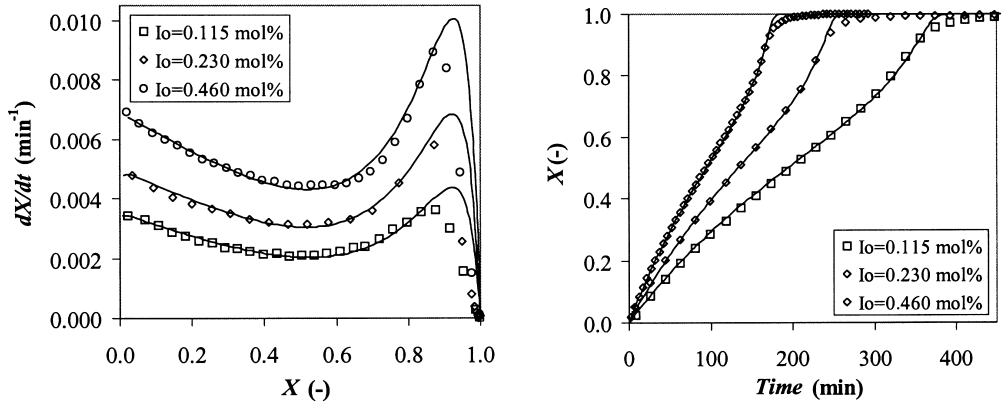

Fig. 4. Evolution of the reaction rate and conversion for the bulk free radical styrene polymerization initiated with Lu256 at 80°C.

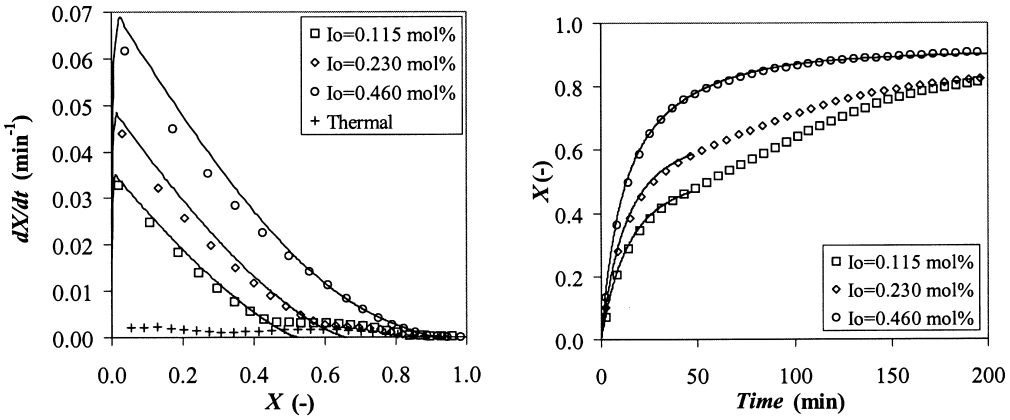

Fig. 5. Evolution of the reaction rate and conversion for the bulk free radical styrene polymerization initiated with Lu256, and thermal polymerization at 110°C.

The styrene was purchased by EniChem (Mantova, Italy) and used without prior treatment. To initiate the polymerization, 2,5-dimethyl-2,5-bis(2-ethylhexanoyl peroxy)-hexane (Lupersol 256) (Akzo Nobel, Deventer, Netherlands) or 2,2′-azobis(isobutyronitrile) (AIBN) (Fluka AG, Buchs, Switzerland) were added.

For the measurements, aluminum crucibles were used (ME-27331, Mettler, Switzerland). In order to avoid any problem of sample mass (gradient of temperature) [28] or oxygen (activation or inhibition) [29], 10 mg of reaction mixture were put in the crucible [30].

The crucibles were put into the calorimeter at 30°C then the oven temperature was set at the selected value. The heating rate was approximately 260°C min^{-1}. The increase of temperature during the gel effect of a styrene polymerization was less than 0.5°C, which ensures isothermality.

The DSC curves were sampled on-line and processed by computer, and from the DSC curves the course of the polymerization was followed [31]. Conversion at different reaction times were calculated from the area between the curve and the baseline, which was obtained by back extrapolation of the straight line, recorded after the end of the polymerization reaction [32,33]. The experimental heat of polymerization is with less than 10% consistent with the literature (-67.5 to -70 kJ mol^{-1}, [26]).

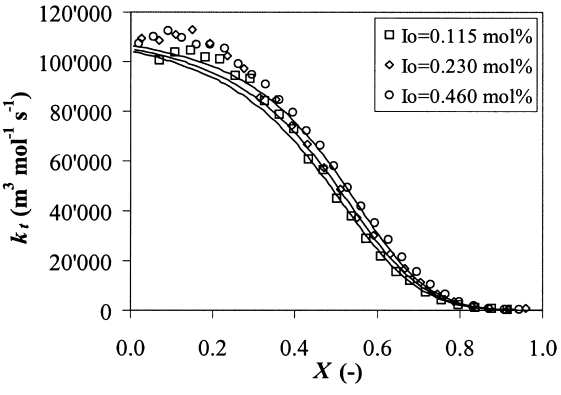

Fig. 6. k_t calculated from the experimental rate of polymerization at 80°C.

The unreacted monomer content was determined by gas chromatography with a Perkin–Elmer GC autosystem (Norwalk, USA) with a Supelco SPB-1 column (Bellefonte, USA).

The average molecular weight of the polystyrene was measured by gel permeation chromatography (GPC) relative to polystyrene standards from Polymer Laboratories (Amherst, USA). A Waters 150 CV model (Milford, USA) equipped with ultrastyragel columns (Waters, pore size 10,000, 1000, 500 and 100 Å) was used with a refractometer and UV absorbance (757 Applied Biosystems, Switzerland) detectors. Tetrahydrofuran was used as solvent.

4. Results and discussion

The half-life time of the Lupersol 256 determined from these DSC curves (Table 3) is in agreement with the data of the literature [34].

As shown on Fig. 3, the influence of the diradical S_n on the simulation is totally negligible due to its small concentration in comparison with the monoradical species (approximately 1000 times smaller). The difference between the two simulations is less than 0.1% for the polymerization rate (dX/dt). The influence on the molecular weight is also less than 0.1%, therefore, for all the simulations presented, the simplified model will be used.

Results of the bulk free radical polymerization of styrene initiated with the bifunctional initiator Lu256 are summarized in Figs. 4 and 5. From the experimental values of dX/dt and by using the kinetic constants and the parameters of the Table 2, the termination constant is calculated with Eq. (11) and presented as a function of the conversion in Fig. 6.

Experimentally, the change of the type of initiator influences very slightly k_t (Fig. 8). This influence is of the same order of magnitude than for the initiator concentration change. Thus, bifunctional initiators are not a particular case for the calculation of the polymerization constants. The effects that will be discussed further are not induced by an unexpected reactivity of the bifunctional initiator.

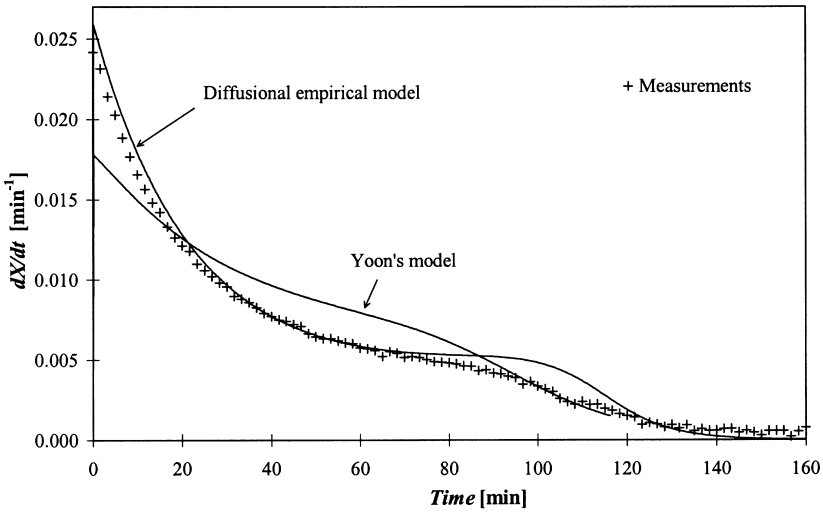

Fig. 7. Experimental rate of polymerization compared with the model of Yoon and the diffusional empirical model. $I_0 = 0.230$ mol%, $T = 100°C$.

The model describes well the polymerization rate between 80 and 100°C. However, one can observe a discrepancy for conversion higher than approximately 80%. This effect can be attributed to a decrease in the propagation rate due to the viscosity of the solution (glass effect).

At 110°C and at the beginning, the reaction rates are in good agreement with the predicted values with $f = 0.8$. This indicates that the initiator has not the expected efficiency at high temperature probably due to another degradation reaction leading to an inactive species. This effect is expressed by a decrease of the experimental rate observed and cannot be attributed to an underestimated decomposition constant. Already at 100°C, the initial reaction is slightly too small. This effect should increase with the temperature.

Then the reaction rates remain sufficiently strong to lead to a complete conversion, which is not the case with the calculated values, which reach a plateau. Indeed, by simulation, for small initiator concentration and high temperature, the decomposition is very fast, leading to a high concentration of radical and a high termination rate. Dead-end type polymerization occurs due to a premature decomposition, resulting in much less than 100% of monomer conversion.

Experimental rate is higher than the simulation due to the fact that the thermal initiation is neglected in this model. One can see in Fig. 5 that for conversion higher or equal to 60%, the experimental reaction rate is following the curve of the thermal polymerization. At 110°C and $t = 50$ min, the residual content of undecomposed initiator is less than 1% of the initial concentration. By increasing the concentration of initiator, the discrepancy is displaced at higher conversions. Even for $I_0 = 0.460$ mol%, the simulation detaches from the experimental curve and predicts a final conversion smaller than 100% (not shown), but the discrepancy occurs at $X = 90\%$.

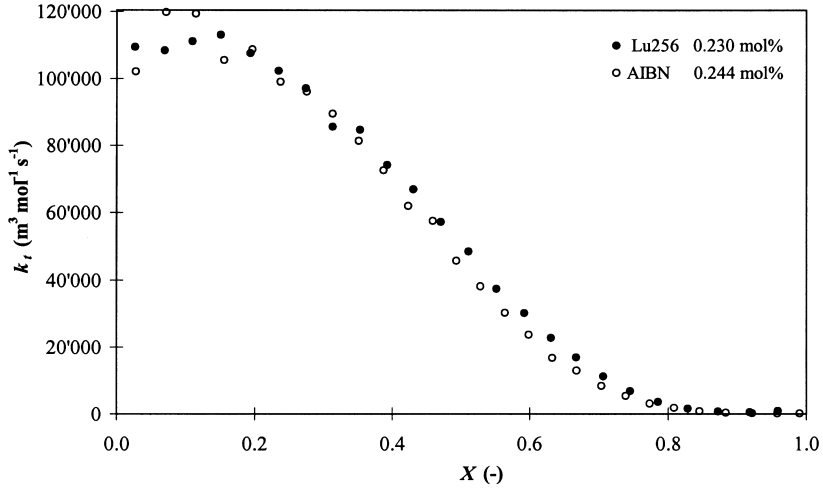

Fig. 8. Comparison between k_t calculated from the experimental polymerization rate initiated with Lu265 and AIBN at 80°C.

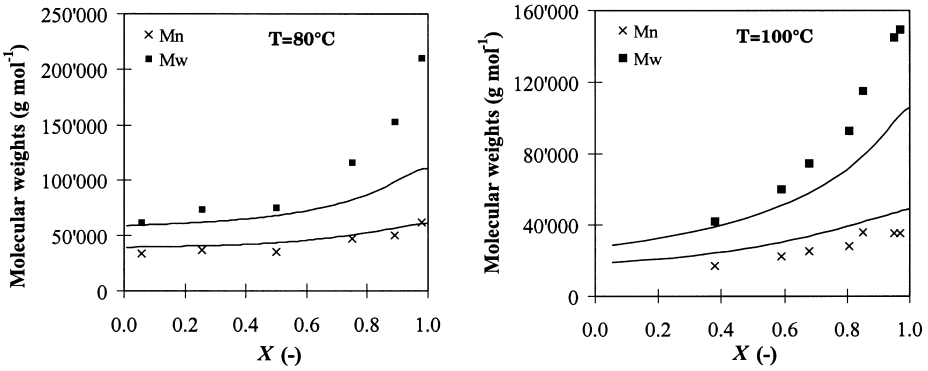

Fig. 9. Average molecular weights for the polymerization of styrene initiated with 0.23 mol% of Lu256; experimental results and simulation.

The predicted termination constants are close to the measured values. As the termination constant is sensitive to the slightest experimental error, it is satisfactory to have a qualitatively good agreement between the model and the measurements. The gel effect is slightly more pronounced (k_t decreases faster) when the initiator concentration decreases. A very important gap between the various k_t is observed at the end of the reaction at 100°C. It is due to the quasi-exhaust of the initiator before the end of the reaction for a concentration of $I_0 = 0.115$ mol%.

The experimental rate of polymerization and a comparison with the model of Yoon and the diffusional empirical model are shown on the Fig. 7. The diffusional empirical model gives a better description of the rate of polymerization.

The molecular weights measured and predicted that are reported in Table 4 indicate a growing polydispersity at high conversions. The average molecular weights given in the Table 4 correspond to complete conversion.

The average number molecular weight $\bar{M}_n$ predicted from the Eq. (15), with an optimized f, and those measured at the end of the reaction, are compared in Table 4. For AIBN, a theoretical value of $\bar{M}_n$ is calculated from the initiator concentration and with $f = 1$. The $\bar{M}_n$ measured is superior to the prediction, which indicates an efficiency factor smaller than 1. If this difference is only due to the efficiency, the ratio of the two values gives the efficiency $f = 0.7$ for the AIBN, which is close to the literature value [35]. For Lu256, one can observe that the measured molecular weights are close to the theoretical values at low temperatures and high initiator concentrations, which makes efficiency factor as close to 1 as possible. For instance, Fig. 10 shows the initiator efficiency calculated [36] from the experimental value of the rate of polymerization and with the QSSA (see Eq. (11), valid for $X < 20\%$). The average initiator efficiency is close to the calculated one. At high temperatures and low initiator concentrations, the difference between predicted and calculated values will increase. This can be explained by the chain transfer, which becomes more important for higher chain length. The latter becomes high when the initiator concentration is small. This could happen by the exhaust of the initiator at high temperature or directly by an initial low concentration.

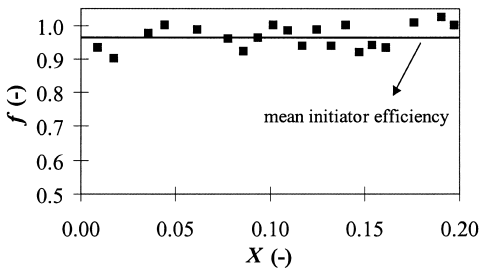

Fig. 10. Initiator efficiency calculated from the experimental rate of polymerization and with the QSSA. $T = 80°C$, $I_0 = 0.230$ mol%.

The experimental mass molecular weights are much higher than the predicted ones (Fig. 9). This can be linked with the non-validity of a k_t constant for all the radicals [37]. A constant k_t dependent on the chain length would give a better result. For long chains, the termination would be smaller than for small active chains due to a restricted mobility [37–42], which leads to an increase of the mass molecular weight and the polydispersity.

5. Concluding remarks

A semi-empirical diffusional model describing the polymerization in batch systems has been developed. Besides the good description of the polymerization kinetics, the model allows the correct prediction of the number-average molecular weight. Discrepancies appear only for very high conversions, high temperatures and low concentrations of the initiator. The polydispersity is underestimated for conversion higher than 70%. The measurements showed that the efficiency factor of the Lu256 for the bulk polymerization of styrene at temperatures between 80 and 100°C is close to 1. For reaction temperature higher than 100°C, thermal initiation must be taken into account. In this case, the efficiency factor seems to decrease to 0.8.

Appendix A. 0, 1st and 2nd moments of the polymeric species

Complete model:

$$R_I = -2k_dI$$

$$R_M = -k_pM(P_t + Q_t + 2S_t)$$

$$R_{\lambda_{P,0}} = R_{P_t} = k_iRM + fk_dZ_t - k_tP_t(P_t + Q_t)$$

$$R_{\lambda_{P,1}} = k_iRM + fk_d\lambda_{Z,1} + k_pMP_t + k_t(2P_t\lambda_{S,1} - (P_t + Q_t)\lambda_{P,1})$$

$$R_{\lambda_{P,2}} = k_iRM + fk_d\lambda_{Z,2} + k_pM(2\lambda_{P,1} + P_t) + k_t(4\lambda_{S,1}\lambda_{P,1} + 2\lambda_{S,2}P_t - (P_t + Q_t)\lambda_{P,2})$$

$$R_{\lambda_{Q,0}} = R_{Q_t} = k_iR_AM + k_d(2fU_t - Q_t) - k_tQ_t(P_t + Q_t)$$

$$R_{\lambda_{Q,1}} = k_iR_AM + k_d(2f\lambda_{U,1} - \lambda_{Q,1}) + k_pMQ_t + k_t(2\lambda_{S,1}Q_t - (P_t + Q_t)\lambda_{Q,1})$$

$$R_{\lambda_{Q,2}} = k_iR_AM + k_d(2f\lambda_{U,2} - \lambda_{Q,2}) + k_pM(2\lambda_{Q,1} + Q_t) + k_t(4\lambda_{S,1}\lambda_{Q,1} + 2\lambda_{S,2}Q_t - (P_t + Q_t)\lambda_{Q,2})$$

$$R_{\lambda_{S,0}} = R_{S_t} = 2k_iR'M + fk_dQ_t - 2k_t(S_t(P_t + Q_t) + S_t^2)$$

$$R_{\lambda_{S,1}} = 2k_iR'M + fk_d\lambda_{Q,1} + 2k_pMS_t - 2k_t(P_t + Q_t)\lambda_{S,1}$$

$$R_{\lambda_{S,2}} = 2k_iR'M + fk_d\lambda_{Q,2} + 2k_pM(2\lambda_{S,1} + S_t) + k_t(4\lambda_{S,1}^2 - 2(P_t + Q_t)\lambda_{S,2})$$

$$R_{\lambda_{U,0}} = R_{U_t} = -2k_dU_t + \frac{k_t}{2}Q_t^2$$

$$R_{\lambda_{U,1}} = -2k_d\lambda_{U,1} + k_t\lambda_{Q,1}Q_t$$

$$R_{\lambda_{U,2}} = -2k_d\lambda_{U,2} + k_t(\lambda_{Q,2}Q_t + \lambda_{Q,1}^2)$$

$$R_{\lambda_{Z,0}} = R_{Z_t} = -k_dZ_t + k_tP_tQ_t$$

$$R_{\lambda_{Z,1}} = -k_d\lambda_{Z,1} + k_t(\lambda_{P,1}Q_t + \lambda_{Q,1}P_t)$$

$$R_{\lambda_{Z,2}} = -k_d\lambda_{Z,2} + k_t(\lambda_{P,2}Q_t + 2\lambda_{P,1}\lambda_{Q,1} + \lambda_{Q,2}P_t)$$

$$R_{\lambda_{M',0}} = R_{M_t} = \frac{k_t}{2}P_t^2$$

$$R_{\lambda_{M',1}} = k_tP_t\lambda_{P,1}$$

$$R_{\lambda_{M',2}} = k_t(P_t\lambda_{P,2} + \lambda_{P,1}^2)$$

Simplified model:

$$R_I = -2k_dI$$

$$R_M = -k_pM(P_t + Q_t)$$

$$R_{\lambda_{P,0}} = R_{P_t} = k_iRM + fk_dZ_t - k_tP_t(P_t + Q_t)$$

$$R_{\lambda_{P,1}} = k_iRM + fk_d\lambda_{Z,1} + k_pMP_t - k_t(P_t + Q_t)\lambda_{P,1}$$

$$R_{\lambda_{P,2}} = k_iRM + fk_d\lambda_{Z,2} + k_pM(2\lambda_{P,1} + P_t) - k_t(P_t + Q_t)\lambda_{P,2}$$

$$R_{\lambda_{Q,0}} = R_{Q_t} = k_iR_AM + 2fk_dU_t - k_tQ_t(P_t + Q_t)$$

$$R_{\lambda_{Q,1}} = k_iR_AM + 2fk_d\lambda_{U,1} + k_pMQ_t - k_t(P_t + Q_t)\lambda_{Q,1}$$

$$R_{\lambda_{Q,2}} = k_iR_AM + 2fk_d\lambda_{U,2} + k_pM(2\lambda_{Q,1} + Q_t) - k_t(P_t + Q_t)\lambda_{Q,2}$$

$$R_{\lambda_{U,0}} = R_{U_t} = -2k_dU_t + \frac{k_t}{2}Q_t^2$$

$$R_{\lambda_{U,1}} = -2k_d\lambda_{U,1} + k_t\lambda_{Q,1}Q_t$$

$$R_{\lambda_{U,2}} = -2k_d\lambda_{U,2} + k_t(\lambda_{Q,2}Q_t + \lambda_{Q,1}^2)$$

$$R_{\lambda_{Z,0}} = R_{Z_t} = -k_dZ_t + k_tP_tQ_t$$

$$R_{\lambda_{Z,1}} = -k_d\lambda_{Z,1} + k_t(\lambda_{P,1}Q_t + \lambda_{Q,1}P_t)$$

$$R_{\lambda_{Z,2}} = -k_d\lambda_{Z,2} + k_t(\lambda_{P,2}Q_t + 2\lambda_{P,1}\lambda_{Q,1} + \lambda_{Q,2}P_t)$$

$$R_{\lambda_{M',0}} = R_{M_t} = \frac{k_t}{2}P_t^2$$

$$R_{\lambda_{M',1}} = k_tP_t\lambda_{P,1}$$

$$R_{\lambda_{M',2}} = k_t(P_t\lambda_{P,2} + \lambda_{P,1}^2)$$

References

[1] Chiu WY, Carrat GM, Soong DS. Macromolecules 1983;16(3):348–57.
[2] Kamath VR. Mod Plast 1981;58:106–10.
[3] Villalobos MA, Hamielec AE, Wood PE. J Appl Polym Sci 1993;50(2):327–43.
[4] Villalobos MA, Hamielec AE, Wood PE. J Appl Polym Sci 1991;42:629–41.
[5] Yoon WJ, Choi KY. J Appl Polym Sci 1992;46(8):1353–67.
[6] Gonzalez IM, Meira GR, Oliva HM. J Appl Polym Sci 1996;59(6):1015–26.
[7] Kim KJ, Choi KY. Chem Engng Sci 1989;44(2):297–312.
[8] Choi KY, Lei GD. AIChE J 1987;33(12):2067–76.
[9] Yoon WJ, Choi KY. Polymer 1992;33(21):4582–91.
[10] Choi KY, Liang WR, Lei GD. J Appl Polym Sci 1988;35:1547–62.
[11] Kim KJ, Choi KY. Chem Engng Sci 1988;43(4):965–77.

[12] Yoon WJ, Choi KY. Polym Engng Sci 1996;36(1):65–77.
[13] Rouge A. Etude de la polymérisation radicalaire du styrène initiée par un amorceur bifonctionnel dans un réacteur tubulaire à recyclage, Diploma work, DC, EPF, Lausanne, 1997.
[14] Luft G, Dorn M. J Macromol Sci—Chem 1988;A25(8):987–98.
[15] Ivanchev SS, Zeherebin YL. Polym Sci USSR 1974;16(4):956–63.
[16] Yerigova SG, Ivanchev SS. Polym Sci USSR 1969;11(9):2377–85.
[17] Luft G, Lim P-C, Pavlakis S, Seidl H. J. Macromol Sci—Chem 1985;A22(9):1183–200.
[18] Prisyazhnyuk AI, Ivanchev SS. Polym Sci USSR 1970;12(2):514–24.
[19] Fried JR. Polymer science and technology, Englewood Cliffs, NJ: Prentice-Hall, 1995.
[20] Kukulj D, Davis TP, Gilbert RG. Macromolecules 1998;31:994–9.
[21] Moad G, Solomon DH. In: Eastmond GC, Ledwith A, Russo S, Sigwalt P, editors. Comprehensive polymer science, 3. Oxford: Pergamon Press, 1989.
[22] Yasukawa T, Murakami K. Polymer 1980;21:1423–6.
[23] Bamford CH, Tipper CFH. Free-radical polymerization, Comprehensive chemical kinetics. Amsterdam: Elsevier, 1976.
[24] Ray WH. J Macrom Sci—Rev Macromol Chem 1972;C8(1):1–56.
[25] Connors KA. Chemical kinetics, New York: VCH, 1990 p. 134.
[26] Brandrup J, Immergut EH. Polymer handbook, 3. New York: Wiley Interscience, 1989.
[27] Duerksen JH, Hamielec AE, Hodgings JW. AIChE J 1967;13(6):1081–6.
[28] Martin JL, Salla JM, Cadenato A, Ramis X. J Therm Anal 1992;38:917–27.
[29] Batch GL, Macosko CW. Thermochim Acta 1990;166:185–98.
[30] Fleury P-A. Polymérisation du méthacrylate de méthyle à haute température. Etude cinétique et caractérisation d'un réacteur tubulaire à recyclage, Thesis 1177, DC, EPF, Lausanne, 1993.
[31] Ebdon JR, Hunt BJ. Anal Chem 1973;45(4):804–6.
[32] Filipovic DM, Petrovic-Dakov DM, Vrhovac LP, Velikovic JS. J Therm Anal 1992;38:709–13.
[33] Malavasic T, Vizovisek I, Lapanje S, Moze A. Makromol Chem 1974;175:873–80.
[34] Technical Bulletin, 1986, Pennwalt-Lucidol Company, Buffalo.
[35] Moad G, Rizzardo E, Solomon DH, Johns SR, Willing RI. Makromol Chem Rapid Commun 1984;5:783–9.
[36] Russell GT, Napper DH, Gilbert RG. Macromolecules 1988;21:2141–8.
[37] O'Neil AG, Torkelson JM. Macromolecules 1999;32(2):411–22.
[38] O'Shaughnessy B, Yu J. Macromolecules 1994;27:5079–85.
[39] O'Shaughnessy B, Yu J. Macromolecules 1994;27:5067–78.
[40] Russell GT, Gilbert RG, Napper DH. Macromolecules 1992;25:2459–69.
[41] Russell GT, Gilbert RG, Napper DH. Macromolecules 1993;26:3538–52.
[42] Scheren PAGM, Russell GT, Sangster DF, Gilbert RG, German AL. Macromolecules 1995;28:3637–49.